Transition flow ion transport: Theory

T. E. Darcie*
Institute for Aerospace Studies, University of Toronto, 4925 Dufferin Street, Downsview, Ontario, Canada M3H 5T6
(Received 12 September 1983; revised manuscript received 16 April 1984)

A new approach is developed to solve the integral Boltzmann equation for the evolving velocity distribution of a source of ions, undergoing electrostatic acceleration through a neutral gas target. The theory is applicable to arbitrarily strong electric fields, any ion- to neutral-mass ratio greater than unity, and is not limited to spatially isotropic gas targets. A hard-sphere collision model is used, with a provision for inelasticity. Both axial and radial velocity distributions are calculated for applications where precollision radial velocities are negligible, as is the case for ion-beam extraction from high-pressure sources and drift tubes operated with strong electric fields.

I. INTRODUCTION

The dynamic flow of charged particles through a neutral gas has received considerable attention in both collision-dominated and collision-free transport systems. In collision-dominated flows the high collision frequency immediately casts the charged and neutral particles into a state of local equilibrium, from which transport properties may be calculated. An applied external electric field perturbs the charged particles from equilibrium and, if this perturbation is slight, techniques similar to the Chapman-Enskog method may be employed.[1,2] In collision-free systems, the charged-particle distribution is altered only by relatively long-range electrostatic forces and theoretical solutions are based on the equations of Laplace or Poisson.[3]

Many practical situations involve the transition between the two aforementioned charged-particle flow regimes. One example, which involves this entire transition, is the coupling of high-pressure ion sources to high-vacuum mass spectrometers. The combined influence of electric fields and ion-molecule collisions, in the pressure transition region, can result in an ion velocity distribution that is unacceptable for efficient mass analysis.[4] Here the ion distribution evolves continuously from a thermally equilibrated "Maxwellian," at the source, into a collision-free, paraxial ion beam at the spectrometer. In order to quantitatively describe this type of ion transport one must abandon familiar concepts such as drift velocity and ion temperature, conveniently permitted in "quasiequilibrium" kinetic theory, and deal with a multidimensional ion-distribution function.

Two types of transition-ion transport can be defined. Isotropic transition ion flow results from the evolution of a localized ion source (e.g., point or infinite-plane source) through spatially isotropic neutral number densities and electric fields. Anisotropic transition (or just transition) ion flow includes spatial variations of ion source, neutral density, and electric field and is the class to which the aforementioned example belongs.

The "linear" Boltzmann equation provides a theoretical framework for this type of transport problem[1] but mathematical complexities, imposed primarily by the many dimensions required, have prevented application to transition problems and limited application to isotropic transition problems. The linear form is derived from the full Boltzmann equation when the ion (test particle) number density is much less than that of the neutrals (field particles). In this case the ion distribution function can be determined by considering only ion-neutral collisions. This "test-particle" assumption has been widely employed in studies involving neutron transport in reactors[5] and ion transport in neutral gases, as first noted by Pidduck.[6] In this case the collision integral is separable into an effective collision frequency and an integral involving a scattering kernel.

Unfortunately, the scattering kernel, for a realistic ion-molecule collision, is too complicated to be applied in evaluation of the velocity distribution function even in nontransition systems. Macroscopic properties (e.g., drift velocity), have been calculated for arbitrary field strengths, mass ratios, and a variety of collisional models using moment methods[7,8] but these methods do not provide velocity distributions and are thereby of no use in transition systems.

The linear Boltzmann equation may be transformed into an integral equation[9–11] which is more amenable to computer solutions. This form has been used by Boffi *et al.*,[12,13] for a one-velocity dimensional analysis of electron conductivity in a neutral gas. The scattering is assumed isotropic in the laboratory frame, as appropriate for electron-atom collisions. Isotropic transition transport is considered by the use of an infinite-plane electron source. An extension of that analysis, for equal-mass ions and neutrals, has been proposed;[14] however, isotropic scattering, in the laboratory frame, is again assumed as is not the case for ion-molecule collisions. The method of successive collisions[15,16] can, in principle, describe transition-ion transport; however, computational difficulties are encountered when a large number of mean free paths are considered.

Velocity distribution functions can be determined using Monte Carlo numerical simulations[8,17] which provide a standard for evaluation of various theoretical approaches. However, since a great deal of physical insight is lost and a large amount of computer time is consumed, another

approach would be preferable.

In this paper a new approach is presented, based on the integral Boltzmann equation, which is applicable to arbitrarily strong electric fields, spatially anisotropic neutral gas targets, and any ion- to neutral-mass ratio greater than unity. A hard-sphere collision model is used since relative velocities are sufficiently high to remove the dominance of polarization, or induced dipole forces. Inelasticity is also considered.

The paper is divided into three sections. Section I presents the general theoretical formulation of the integral Boltzmann equation and collisional model. Section II applies the formalism of Sec. I to configurations resulting in highly nonthermal ion distributions. In Sec. III two specific configurations are studied demonstrating both isotropic and anisotropic transition flow. One configuration is the acceleration of a nearly thermal ion source through a spatially isotropic, low-density neutral target, as encountered in a low-pressure, strong-field drift tube. The second is the acceleration of a thermal ion source through a high-pressure-ratio, free jet expansion. This is encountered when ions are formed at high pressure and enter a vacuum with neutrals through an orifice.

II. GENERAL THEORY

The ion distribution function $f(\vec{x},\vec{v},t)$ is governed by the Boltzmann equation[1,18]

$$\left[\frac{\partial}{\partial t}+\vec{v}\cdot\vec{\nabla}_{\vec{x}}+\frac{\vec{F}(\vec{x},t)}{m}\cdot\vec{\nabla}_{\vec{v}}\right]f(\vec{x},\vec{v},t)=\left[\frac{\partial f}{\partial t}(\vec{x},\vec{v},t)\right]_{\text{coll}}+Q(\vec{x},\vec{v},t)\,. \quad (1)$$

$\vec{F}$ is an externally applied conservative force, $Q(\vec{x},\vec{v},t)$ is an externally applied ion source, and $f(\vec{x},\vec{v},t)d\vec{x}\,d\vec{v}$ is the number of ions within element $d\vec{x}=dx\,dy\,dz$, centered at $\vec{x}$, with velocity within element $d\vec{v}$, centered at $\vec{v}$. $(\partial f/\partial t)_{\text{coll}}$ is the collision integral and, if ion-ion collisions may be neglected, can be expressed as[1]

$$\left[\frac{\partial f}{\partial t}\right]_{\text{coll}}=\int K[\vec{v}\,'\rightarrow\vec{v}]f(\vec{v}\,')d\vec{v}\,'-\nu(\vec{v})f(\vec{v})\,, \quad (2)$$

where, for hard-sphere collisions

$$K[\vec{v}\,'\rightarrow\vec{v}]=S\int F_0(\vec{v}\,'_0)\delta(\vec{A})\delta(B)d\vec{v}_0d\vec{v}\,'_0 \quad (3)$$

is the scattering kernel and

$$\nu(\vec{v}\,')=S\int F_0(\vec{v}\,'_0)\delta(\vec{A})\delta(B)d\vec{v}\,'_0\,d\vec{v}_0d\vec{v} \quad (4)$$

is the effective collision frequency. Subscript 0 denotes neutral and primes indicate precollision conditions. For brevity $f(\vec{v})$ and $F_0(\vec{v}_0)$ replace $f(\vec{x},\vec{v},t)$ and $F_0(\vec{x}_0,\vec{v}_0,t)$ for ion and neutral velocity distribution functions, respectively. When ion-ion collisions are negligible, the neutral distribution $F_0(\vec{v}\,'_0)$ is unaltered by ion-neutral collisions. Also

$$S=\tfrac{1}{2}\sigma^2(m+m_0)^2mm_0\,, \quad (5)$$

$$\delta(\vec{A})=\delta(m\vec{v}+m_0\vec{v}_0-m\vec{v}\,'-m_0\vec{v}\,'_0)\,, \quad (6)$$

$$\delta(B)=\delta(mv^2+m_0v_0^2-mv^2-m_0v_0^2)\,, \quad (7)$$

where σ is the sum of ion and neutral radii and m,m_0 are the ion and neutral masses, respectively. δ is the Dirac δ function. $K[\vec{v}\,'\rightarrow\vec{v}]$ may be regarded as a partial collision frequency since $K[\vec{v}\,'\rightarrow\vec{v}]d\vec{v}\,'$ is the number of collisions, per unit time, of test particles with initial velocities between $\vec{v}\,'$ and $\vec{v}\,'+d\vec{v}\,'$ that are scattered into velocities between $\vec{v}$ and $\vec{v}+d\vec{v}$.

Equation (1) can be converted into an integral equation by using a change of variable to change the substantial derivative into a total derivative and integrating. Thus for a constant force $\vec{F}$ and steady-state solutions[9,19]

$$f[\vec{x},\vec{v}]=\int_0^\infty d\tau\exp\left[-\int_0^\tau\nu[\vec{x}(\tau'),\vec{v}(\tau')]d\tau'\right]\times G[\vec{x}(\tau),\vec{v}(\tau)]\,, \quad (8)$$

where

$$G(\vec{x},\vec{v})=\int K[\vec{x},\vec{v}\,'\rightarrow\vec{v}]f(\vec{x},\vec{v}\,')d\vec{v}\,'+Q(\vec{x},\vec{v})\,, \quad (9)$$

$$\vec{v}(\tau)=\vec{v}-\vec{F}\tau/m\,, \quad (10)$$

$$\vec{x}(\tau)=\vec{x}-\vec{v}\tau+\vec{F}\tau^2/(2m)\,. \quad (11)$$

$G[\vec{x}(\tau),\vec{v}(\tau)]$ represents all possible events (source creation or collision) that occur at time τ that would result in the population of the phase-space element $d\vec{x}\,d\vec{v}$ at $\vec{x},\vec{v}$. The exponential is an attenuation factor to account for subsequent collisions as those test particles move along their trajectories from $\vec{x}(\tau),\vec{v}(\tau)$ to $\vec{x},\vec{v}$. The integration over τ is a summation over all possible past times that can effect $f(\vec{x},\vec{v})$.

Various collision models have been used in moment method calculations[7] where the velocity distribution is not determined. The most widely used interaction corresponds to the inverse fifth-power force law. These "Maxwell molecules" represent the induced dipole polarization force between ions and molecules and result in constant mean free time scattering. As the relative velocity increases, the influence of polarization decreases and hard-sphere collisions, characterized by a constant mean free path, become dominant. At the relative energies involved in this study, polarization can be neglected. When an ion is forced through its parent gas, the symmetry of charge affinities allows a resonance charge transfer to occur. In this case each collision effectively stops the ion and leaves a neutral with the entire initial energy. This has been treated[20] but is of little concern here where large charge-affinity differences will be assumed. Hard-sphere collisions, which have already been introduced in Eqs. (2) and (3), but with a provision for inelasticity would be a suitable collisional model.

For many ion-neutral problems, ions have undergone considerable acceleration and have speeds much greater than neutrals. In this case, the neutral distribution appears frozen to incident ions and a stationary distribution will apply

$$F_0(\vec{v}\,'_0)=N(\vec{x})\delta(\vec{v}\,'_0)\,. \quad (12)$$

The neutrals will be allowed to recoil, to conserve momentum and energy, and to maintain scattering aniso-

tropy. $N(\vec{x})$ is the physical space number density of target molecules since

$$\int F_0(\vec{v}\,'_0)d\vec{v}\,'_0=N(\vec{x})\ . \tag{13}$$

Most ion-molecule collisions are not elastic because of the many internal degrees of freedom in organic molecules of interest. It is convenient to introduce a parameter p that will help explain the effect of this inelasticity. Since for stationary targets the entire initial energy is that of the incident ion, let p represent the fraction of this incident energy remaining in translational motion of the ion and neutral after the collision. That is to say $(1-p)$ times the incident ion energy is converted into internal vibration, rotation, or electronic excitation. Integration of Eq. (3) results in

$$K[\vec{v}\,'\rightarrow\vec{v}]=\frac{\sigma^2}{2}\frac{N(1+r)}{B}\times\delta\left[\left[\vec{v}-\vec{v}\,'\frac{r}{1+r}\right]^2-v^2\left[\frac{p(1+r)-r}{(1+r)^2}\right]\right]. \tag{14}$$

B is a normalization constant to compensate for the addition of p, and will be discussed later in this section, and the mass ratio $r=m/m_0$. With $p=1$, or for perfectly elastic collisions, this kernel is equivalent to one developed by Whipple.[21] The parameter p describes inelasticity by allowing the absorption of a fixed amount of energy regardless of the collisional impact parameter. This will be referred to as symmetric inelasticity. In actuality a head on collision would be more inelastic than a grazing collision. Another parameter, ϵ, is introduced later to describe this asymmetric inelasticity.

The normalization constant B, and the collision frequency $\nu(\vec{v})$ can be determined from Eq. (4):

$$B=[p(1+r)-r]^{1/2}\ , \tag{15}$$

$$\nu(\vec{x},\vec{v})=\pi\sigma^2N(\vec{x})v=\Sigma_s v=\frac{v}{\lambda}\ , \tag{16}$$

where λ is the mean free path and Σ_s is the macroscopic cross section.

III. APPLICATION OF INTEGRAL EQUATION

Exact solutions of the integral transport equation, for a transition problem with anisotropic scattering, would involve six velocity variables (three precollision and three postcollision) and one position variable. Some loss of generality is essential. Considerable simplification results if the axial component of precollision velocity is much larger than the transverse v_r'. Each collision can then be described approximately by one precollision, v_x' and two postcollision, v_x and v_r, velocity components.

This approach is ideal for applications in which the ion trajectories are paraxial such as for large mass ratios, strong fields, or axially decreasing target-number density. Provided that on the average, v_r'/v_x' is less than approximately 0.2, where a small-angle approximation is reasonable, an accurate distribution of axial velocities is expected. One does expect, however, to underestimate the radial diffusion.

A constant electric field (E) is applied in the x direction and an infinite-plane ion source, with velocity distribution $Q(v_x,v_r)$, is applied at $x=0$. These source ions accelerate in the positive x direction and experience collisions with the neutrals of number density $N(x)$. Collisions occur at the frequency $\nu(x,v_x,v_r)$ and result in velocities given by $K[x,v_x'\rightarrow v_x,v_r]$. For this application Eq. (8) can be expressed as

$$f[x,v_x,v_r]=f_s[x,v_x,v_r]+f_c[x,v_x,v_r]\ , \tag{17}$$

where

$$f_s[x,v_x,v_r]=\int_0^\infty d\tau e^{-I(\tau)}Q[x(\tau),v_x(\tau),v_r]\ , \tag{18}$$

$$f_c[x,v_x,v_r]=\int_0^\infty d\tau e^{-I(\tau)}\int_v K[x(\tau),v_x'\rightarrow\vec{v}(\tau)]\times f[x(\tau),\vec{v}\,']d\vec{v}\,'\ , \tag{19}$$

$$\exp[-I(\tau)]=\exp\left[-\pi\sigma^2\int_0^\tau N[x(\tau')]v(\tau')d\tau'\right]. \tag{20}$$

f_s represents ions directly from the source, depleted by the attenuation factor, Eq. (20). f_c represents the contribution to f from all collisions.

Restriction of the source to the $x=0$ plane and the problem to a semi-infinite region places restriction on the limits of integration of τ in Eq. (19). The time τ represents the time for which an ion must accelerate between its last collision and its appearance as part of $f(x,v_x,v_r)$. The distance $x(\tau)$ is the corresponding distance through which the ion traveled. No ion can be allowed to contribute to $f(x,v_x,v_r)$ if $x(\tau)$ places its last collision on the negative x side of the source. Rather than include this effect explicitly in the limit of τ integration, multiplication of $f[x(\tau),v_x',v_r']$ by a nondimensional unit step function will eliminate such a contribution. The τ integral in Eq. (19) can be evaluated by making use of the δ function.

Let

$$K[x(\tau),v_x'\rightarrow v_x(\tau),v_r]=\sigma^2N[x(\tau)](1+r)\delta[g(\tau)]/2\ , \tag{21}$$

where

$$g(\tau)=(\gamma\tau/2)^2+(v_x'\gamma a-v_x\gamma)\tau+v^2-2v_xv_x'a+v_x'^2b\ ,$$
$$\gamma=2F/m=2eE/m\ , \tag{22}$$
$$a=r/(1+r),\quad b=(r-1)/(r+1)\ .$$

The roots of $g(\tau)$ are

$$\tau=2\{v_x-v_x'a\pm[(v_x')^2(a^2-b)-v_r^2]^{1/2}\}/\gamma\ . \tag{23}$$

These roots can be understood from Fig. 1 where the mass ratio $r=1$ and the initial velocity is v_x'. Any final velocity must lie somewhere on the surface of the solid sphere. An ion can populate the distribution at point P from either of two possible collisions, A or B. For $v_x(B)<v_x(A)<v_x(P)$, the ion at A must accelerate for a time τ_A, and the ion at B for a time τ_B, to populate $f(x_p,v_{xp},v_{rp})$.

For point Q, only collision B can serve to populate f. In this case the time τ_A predicted by the negative root in

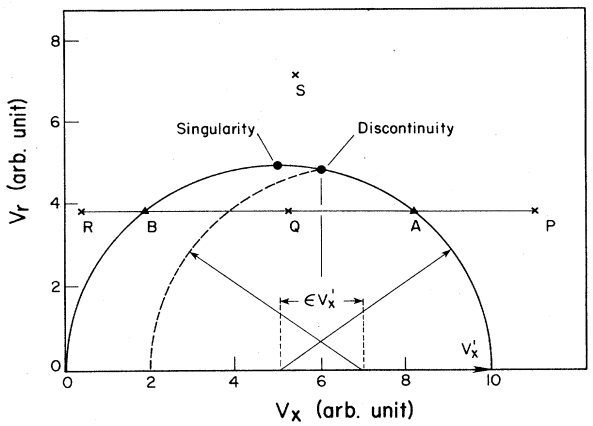

FIG. 1. Scattering kernel for $r=1$ ($a=1/2, b=0$) for exact hard-sphere collision (solid line) and nonsingular discontinuous model (dashed line). Initial ion velocity $v_x'=10$ and $\epsilon=0.2$.

Eq. (23) becomes negative and is then outside the limits of τ integration in Eq. (19).

For the point R, no collision (for v_x' as shown) can contribute. In this case both τ_A and τ_B are negative.

The point S has a radial component greater than any possible outcome of the collision from v_x', thus no contribution is possible. In fact, for $r=1$, no contribution is possible unless $v_r \leq v_x'/2$. If this is not maintained the square root in Eq. (23) becomes imaginary and no real contribution is obtained.

The integration over the quadratic δ function requires the derivative of the quadratic, evaluated at the roots, to be nonzero. When the radical in Eq. (23) is 0, the integrand becomes singular as shown in Fig. 1. This singularity can be eliminated by replacing the continuous kernel, shown as the solid curve, by a discontinuous approximation (dotted line). Since head-on collisions should be less elastic than grazing collisions, the most straightforward removal of the singularity is to translate the wide angle scattering, or reverse collision, portion of the kernel sphere by some small fraction ϵ of the initial ion velocity v_x'. The singularity may then be avoided in a fashion that approximates an asymmetric inelasticity. Restriction of the limits of $\vec{v}\,'$ integration in Eq. (19) confines the contributions to the distribution to be from the appropriate portion of the discontinuous kernel.

Thus for forward collisions Eqs. (22) and (23) still apply, but for reverse collisions

$$K_r[x(\tau),v_x' \rightarrow v_x(\tau),v_r]=\sigma^2 N(x(\tau))(1+r)\delta(g_r(\tau))/2 , \tag{24}$$

where

$$\begin{aligned} g_r(\tau)&=(\gamma\tau/2)^2+(v_x'\gamma c-v_x\gamma)\tau+v^2-2v_x v_x' c+v_x'^2 d , \\ c&=r/(1+r)+\epsilon , \\ d&=[r/(1+r)+\epsilon]^2-(1+r)^{-2} . \end{aligned} \tag{25}$$

The appropriate roots, or collision times of Eqs. (23) and (25) are

$$\tau_f=2\{v_x-v_x' a-[v_x'^2(a^2-b)-v_r^2]^{1/2}\}/\gamma , \tag{26}$$

$$\tau_r=2\{v_x-v_x' c+[v_x'^2(c^2-d)-v_r^2]^{1/2}\}/\gamma . \tag{27}$$

This discontinuous approximation of the kernel sphere has a smaller surface area than the exact sphere and hence is in violation of the principle of detail balance. The probability density on the discontinuous kernel must be increased by multiplying the reverse kernel, Eq. (24), by

$$A=\frac{2+\epsilon(1+r)}{2-\epsilon(1+r)} . \tag{28}$$

The two constants, A and B, and inelasticity parameters ϵ and p, can be used simultaneously to describe a fairly general model of an inelastic collision. ϵ and A describe a spherically asymmetric energy absorption, and p and B describe a symmetric absorption. Equation (19) is then factored into forward and reverse contributions:

$$f_c[x,v_x,v_r]=f_f[x,v_x,v_r]+f_r[x,v_x,v_r] , \tag{29}$$

where, if restricted to only asymmetric inelasticity ($p=1$),

$$\begin{aligned} f_f[x,v_x,v_r]&=\sigma^2\frac{r+1}{2} \\ &\times\int_{v_f'}\frac{N(x(\tau_f))e^{-I(\tau_f)}}{|g_f'(\tau_f)|} \\ &\times f(x(\tau_f),\vec{v}\,')U(x(\tau_f)/L)d\vec{v}\,' , \end{aligned} \tag{30}$$

$$\begin{aligned} f_r[x,v_x,v_r]&=\sigma^2\frac{r+1}{2}A \\ &\times\int_{v_r'}\frac{N(x(\tau_r))e^{-I(\tau_r)}}{|g_r'(\tau_r)|} \\ &\times f(x(\tau_r),\vec{v}\,')U(x(\tau_r)/L)d\vec{v}\,' , \end{aligned} \tag{31}$$

from Eqs. (22) and (25),

$$g_f'(\tau_f)=\gamma^2\tau_f/2+v_x'\gamma a-v_x\gamma , \tag{32}$$

$$g_r'(\tau_r)=\gamma^2\tau_r/2+v_x'\gamma c-v_x\gamma . \tag{33}$$

The appropriate limits of $\vec{v}\,'$ integration are presented in the Appendix. If v_x^*, v_r^* are upper limits and v_x^0 is the lower limit,

$$\int_{v'} d\vec{v}\,'=2\pi\int_0^{v_r^*} v_r' dv_r' \int_{v_x^0}^{v_x^*} dv_x' . \tag{34}$$

The attenuation factor, Eq. (20), can be integrated directly when $N(x)$ is constant but for other $N(x)$ numerical integration is necessary.

Any convenient ion-source velocity distribution $Q(v_x,v_r)$ may be used. To maintain simplicity and generality the ellipsoidal distribution[22] is ideal:

$$Q[x,v_x,v_r]=\frac{Q_0\beta_r\beta_x^{1/2}}{\pi^{3/2}}e^{-\beta_r v_r^2}e^{-\beta_x(v_x-v_0)^2}\delta(x) , \tag{35}$$

where β_x and β_r can be interpreted as inverse characteristic temperatures, v_0 is the average axial velocity, and $\delta(x)$ restricts the source to the effective source plane. Q_0 is the flux of ions crossing the effective source plane per second, per unit area. The source contribution may be evaluated from Eq. (18):

$$f_s[x,v_x,v_r]=\frac{Q_0\beta_r\beta_x^{1/2}}{\pi^{3/2}(v_x^2-\gamma x)^{1/2}} \times e^{-\beta_r v_r^2} e^{-\beta_x[v_x(\tau_0)-v_0]^2} e^{-I(\tau_0)}, \quad (36)$$

where

$$\tau_0=2[v_x-(v_x^2-\gamma x)^{1/2}]/\gamma . \quad (37)$$

The problem of obtaining the distribution function has been reduced to that of solving an integral equation containing three contributions:

$$f[x,v_x,v_r]=f_s[x,v_x,v_r]+f_f[x,v_x,v_r]+f_r[x,v_x,v_r] . \quad (38)$$

Equation (38) most closely resembles a Volterra equation, of the second kind, and is inhomogeneous because of the f_s term. The main problem is that in f_f (and f_r), the value of $f(x(\tau_f))$ must be known [or $f(x(\tau_r))$] where $x(\tau_f)$ depends not only on v_x' but on v_x and v_r. This interdependence defies solution by integral transform methods, even in algebraically less complicated equations.[23]

Advantage must be taken of the fact that the distribution function evolves, from a known source distribution at $x=0$, in a continuous manner along the positive x axis. For a mass ratio of greater than unity, there can be no contribution to the distribution at x from any point downstream of x. The entire region of solution can then be subdivided into slabs of increasing x, and the solution within each slab will depend only on the distribution within the current slab, and all upstream slabs. If the x increments are small, the distribution function at any slab can be approximated by the distribution function at the previous slab. An iterative procedure may then be employed to refine this approximation.

The integration over v_x' and v_r' with variable limits presents an arduous task for a computer if a conventional numerical integration routine is used. This problem can be overcome by using the rather powerful Gaussian quadrature.[24,25] Each quadrature abscissa corresponds to an upstream value of the distribution function. The distribution is determined at each point by summing many contributions from upstream points:

$$f[x,v_x,v_r]=f_s[x,v_x,v_r]+\pi\sigma^2(r+1)\sum_i\sum_j H_iH_jW(\eta_i)Z(\xi_j)N(x(\tau_{fj}))\frac{e^{-I(\tau_{fj})}}{|g_f'(\tau_{fj})|} \times f[x(\tau_{fj}),v_{xj}',v_{ri}']U(x(\tau_{fj})/L)+A[\cdots(\tau_r)] . \quad (39)$$

The term $[\cdots(\tau_r)]$ is identical to the previous term except τ_r replaces τ_f. $W(\eta),Z(\xi)$ transform the v_r',v_x' integrations into the interval -1 to $+1$. The quadrature abscissa are η_i,ξ_j and the weighting coefficients H_i,H_j. A description of the computer program is presented in Ref. 19.

IV. APPLICATIONS

A. Uniform target—isotropic transition transport

When a low-energy ion source is accelerated through a spatially isotropic neutral gas target, the mean free path λ can be used as a distance unit. The electric field and position appear only in combinations of $E\lambda$ and x/λ, respectively, in Eq. (39). Solutions thereby depend only on $E_c=E\lambda$ (volts per mean free path), and the number of mean free paths, or average number of collisions, $z=x/\lambda$. The cross section σ defines λ but is not required for solutions in terms of E_c and z.

The assumption of negligible precollision radial velocity (v_r') results in underestimating the radial diffusion of ions and a poor approximation to the radial distribution. However, for large mass ratios, where the axial velocity (v_x') is much greater than v_r', neglecting v_r' does not significantly alter the distribution of postcollision axial velocities. In such cases, the axial distributions should be quite accurate.

Results are presented for protonated dimethyl-sulfoxide ions ($DMSOH^+$) and a nitrogen-gas target. These ions ($m=79$) can be easily formed using an atmospheric-pressure chemical-ionization ion source, as demonstrated in experimental corroboration of these predictions.[19] Results are also presented for potassium ions ($m=39.1$ amu) because the many previously published drift-tube investigations of potassium or argon ($m=39.9$) ions.

Figure 2 shows the axial velocity distribution evolution, for a mass 79-amu ion and 28-amu neutral, with $E_c=8$ V per mean free path. The source distribution, with a relative height of 192, accelerates and is attenuated by collisions, forming a thermalized distribution at lower energy. After 3.2 mean free paths the source height is attenuated by $\exp(-3.2)$ to a relative height of 8.0. After 8.0 mean free paths, and 64-V potential difference, very few source ions have not collided and subsequent changes in the distribution are insignificant. In all cases the source evolves directly into the terminal distribution, with no intermediate distribution. The distribution at any position can be described by the superposition of source, and thermalized contributions.

Two factors which most strongly influence the velocity distribution are the mass ratio and electric field strength. Terminal axial velocity distributions for $E_c=8$ V, ion mass $m=39.1$ amu (potassium) and various mass ratios are presented in Fig. 3. For $r=1$ the distribution should

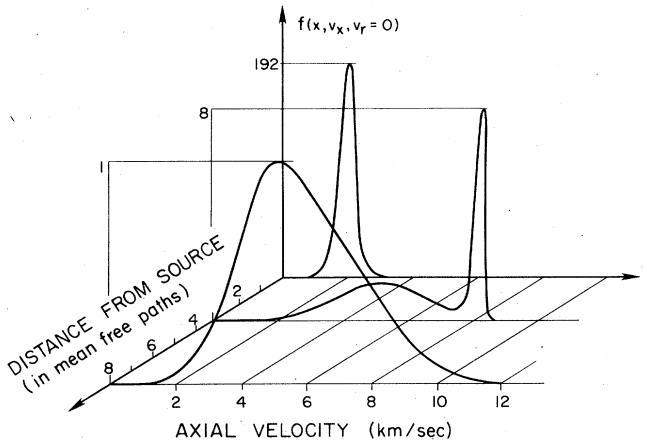

FIG. 2. Axial velocity distribution evolution through uniform gas target. $m=79$ amu, $r=2.82$, $E_c=8$ V.

extend to negative axial velocity; however, neglecting the precollision radial velocity removes this possibility. Some error in the shape of the low-energy tail is also expected for $r=2$ and 3. The magnitude of this error can be estimated by comparing drift velocities with those obtained by Monte Carlo methods.[17] For mass ratio $r=1$ the predicted drift velocity was in excess by 16%. For higher mass ratios the agreement improved such that for $r=3$ the excess was 6.9%.

Although unable to predict axial and radial distributions, for isotropic targets, this procedure can provide the essential features of the transition from an arbitrary source to a terminal distribution (Fig. 2). A reasonable approximation to the axial distribution is obtained for mass ratios greater than approximately 2.

Asymmetric inelasticity, as introduced via parameter ϵ, has little influence on the distribution function in comparison to the mass ratio and electric field strength. Symmetric inelasticity p would have less effect and therefore was not investigated.

B. Free jet target—Anisotropic transition transport

In a free jet expansion the neutral number density decreases as the inverse square of distance from the orifice.[26] If ions are introduced into vacuum through this pressure transition, the ion-flow regime changes from collision dominated to collision free in as little as 1 cm. The importance of an applied electric field increases as the collision dominance decreases and the resultant distribution of ion velocities will determine how efficiently these ions may be analyzed by a mass spectrometer.

An infinite-plane gas target is used with density defined as on the centerline of a free jet expansion, where for a diatomic gas[26]

$$N(x)/N_0=0.089(D/x)^2 . \tag{40}$$

The high-pressure neutral number density is N_0 and the orifice diameter is D. The low-energy ion source is applied a small distance x_0 downstream from $x=0$ and accelerated, by an electric field of strength E, to any downstream point. Results are strongly dependent on ion-molecule hard-sphere collision cross sections, mass ratios, and electric field strengths.

Comparison with experiment is possible using $DMSOH^+$ ions and a nitrogen-gas expansion. Results[19] show excellent agreement for an ion-molecule cross section $\sigma=3.6$ Å.

Figures 4(a)—4(d) show the evolving source (a) accelerated ($E=100$ V/cm) through a nitrogen free jet expansion where $N_0=3.26\times10^{19}$ cm^{-3} and $D=0.005\,08$ cm. The ion source is located at $x_0=0.025$ cm where the ion-molecule mean free path is 0.0027 cm. Collisions dominate up to (b), 0.0130 cm from x_0. The source is rapidly attenuated by collisions in which the precollision radial velocity is not negligible, resulting in the maxima (marked " + ") displaced from the v_x axis. Further from the source the mean free path increases and the axial electric field results in highly paraxial trajectories. At (c), 0.220 cm from source, and (d), 0.379 cm from the source, the mean free paths are 0.256 and 0.696 cm, respectively. Neglecting initial radial velocities is a valid assumption here and both axial and radial distributions should be quite accurate.

The increments opposite v_x,v_r axes represent 1-eV energy increments and the asymmetric inelasticity parameter used was $\epsilon=0.2$. The flux of ions crossing the source plane is $Q_0=10^{10}$ cm^{-2}s^{-1}.

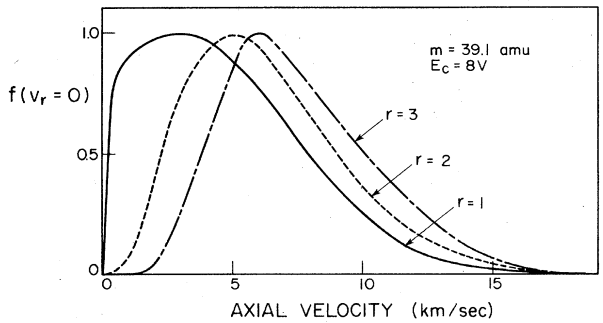

FIG. 3. Axial velocity distributions for various mass ratios and a uniform target; $m=39.1$ amu, $E_c=8$ V.

V. CONCLUSIONS

The integral Boltzmann equation has been solved to determine the evolving velocity distribution of a source of ions, electrostatically accelerated through a spatially anisotropic neutral gas target. The method is ideally suited to configurations resulting in highly paraxial ion trajectories, and is applicable to a wide range of problems, such as ion-beam extraction from high-pressure sources and ion-beam scattering by background molecules.

Experiments[19] show excellent agreement between predicted and measured axial distributions despite assuming negligible precollision radial velocities. This assumption results in underestimating the radial diffusion of ions in all cases but a good approximation of the radial distribution is obtained for configurations resulting in highly paraxial trajectories, such as ion extraction from free jet expansions. The effects of mass ratio, electric field

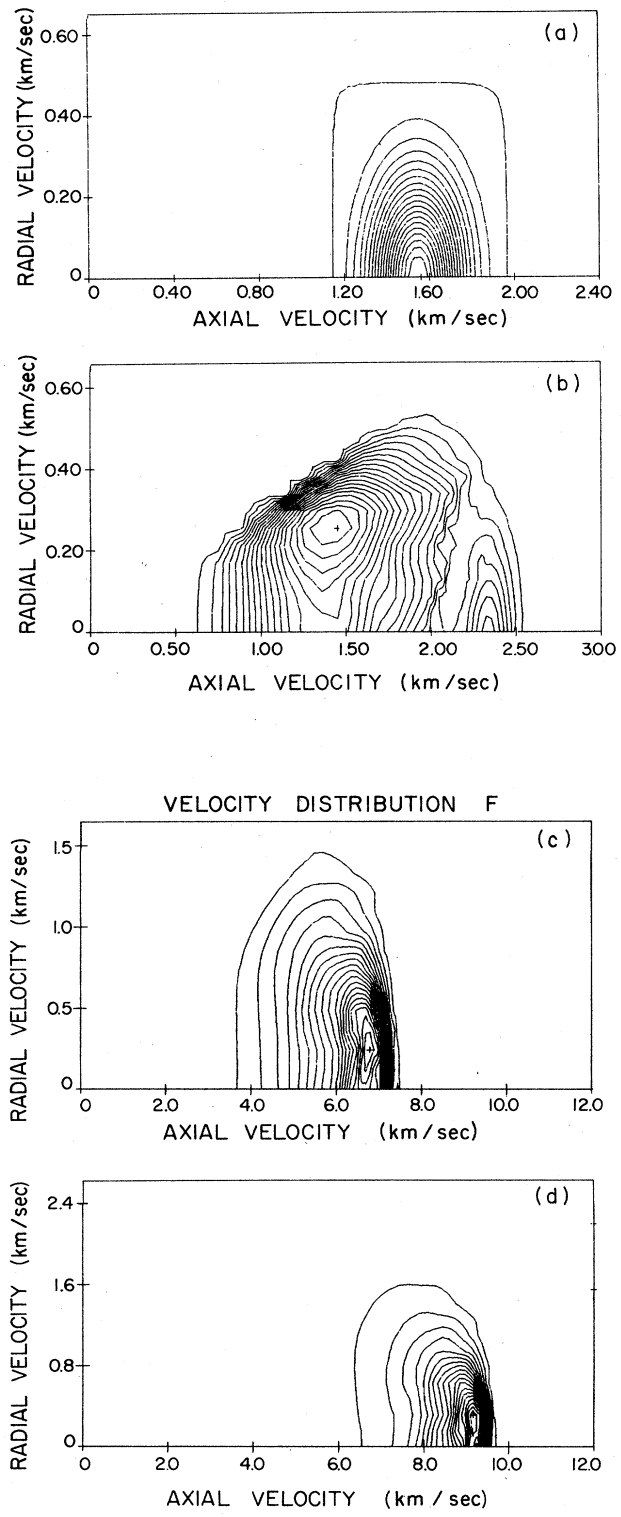

FIG. 4. Evolution of velocity distribution for ions extracted through free jet expansion. Figure 5(a) is the ellipsoidal source defined 0.025 cm downstream from orifice. The maximum height (MH) is 1.8×10^{-9} and the contour interval (CI) is 5.92×10^{-11} (units of s^3cm^{-6}). (b) is 0.0130 cm downstream from (a); MH is 1.59×10^{-10} and CI is 7.93×10^{-12}. (c) is 0.220 cm from (a); MH is 3.67×10^{-12} and CI is 1.84×10^{-13}. (d) is 0.379 cm from (a); MH is 2.77×10^{-12} and CI is 1.38×10^{-13}.

strength, spatial variation of neutral number density, and inelasticity were investigated for quasi-hard-sphere collisions. Inelasticity has little influence on the velocity distribution, compared to the other three parameters.

The incorporation of the position variable provides a more general basis for drift-tube—type experiments. Conventional drift-tube studies require hundreds of collisions to remove any spatial variation and are thereby limited to low-field strengths, where the dominant interaction is through polarization, or to atomic species, where fragmentation does not occur. Since this theory predicts the evolution of a low energy source distribution, a terminal distribution need not be attained and only a few collisions, at lower energies, are required. Hard-sphere collision cross sections can be obtained, for species that would fragment under conventional drift-tube conditions, by simply accelerating the ions through a neutral expansion into vacuum and analyzing the resultant distribution of energies.

ACKNOWLEDGMENTS

I am indebted to my thesis supervisor, Dr. J. B. French of the University of Toronto Institute for Aerospace Studies. This research was supported through the Canadian Natural Sciences and Engineering Research Council, under Grant No. A2731.

APPENDIX: LIMITS OF INTEGRATION

Limits of integration in Eqs. (30) and (31) are determined by several criteria. The maximum velocity attained by an ion leaving the source at $x=0$, with velocity $v_{x_{max}}^2$, is an upper limit to the precollision axial velocity

$$v_x^* = (\gamma x + v_{x_{max}}^2)^{1/2} . \tag{A1}$$

Since precollision radial velocities are assumed negligible, the v_r' integration has an upper limit determined by the kernel (Fig. 1):

$$v_r^* = [(1+r)^{-2} - \epsilon^2/4]^{1/2} v_x^* = u v_x^* . \tag{A2}$$

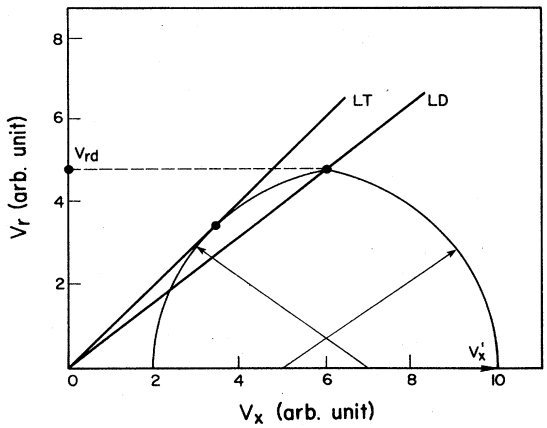

FIG. 5. Regions with different limits of integration for $r=1$, $\epsilon=0.2$, $v_x=10$.

A lower limit to v_x' can be established since no ion can contribute to $f(x,v_x,v_r)$ if v_r is greater than v_{rd} (Fig. 5):

$$v_x^0 = v_r/u \ . \tag{A3}$$

Other upper and lower v_x' limits, which differ for forward and reverse collisions, restrict integration to appropriate τ intervals.

(i) *Forward collisions.* For any point (v_x,v_r) and increasing v_x', the value of τ_f in Eq. (26) can become negative. This upper limit is, for $r>1$,

$$v_x^* = \{v_x a - [(v_x a)^2 - v^2 b]^{1/2}\}/b \tag{A4}$$

and for $r=1$,

$$v_x^* = v^2/v_x \ . \tag{A5}$$

No forward contribution is possible from any point between the line of discontinuities (LD) (Fig. 5), and the v_r axis. The equation of this line is

$$v_x = v_r\{a/u + [(a^2-b)/u^2 - 1]^{1/2}\} \ . \tag{A6}$$

(ii) *Reverse collisions.* No reverse contribution is possible between the line of tangents (LT) and the v_r axis. The equation of line LT is

$$v_x = v_r d^{1/2}/\mathrm{s} \ . \tag{A7}$$

In the region between LD and the v_x axis the lower limit to v_x' is given by Eq. (A3) but to ensure positivity of τ_r [Eq. (27)] an upper limit is

$$v_x^* = \{v_x c + [(v_x c)^2 - v^2 d]^{1/2}\}/d \ . \tag{A8}$$

Between LT and LD the upper limit is unchanged but the lower limit, Eq. (A3), must be replaced by

$$v_x^0 = \{v_x c - [(v_x c)^2 - v^2 d]^{1/2}\}/d \ . \tag{A9}$$

*Present address: AT&T Bell Laboratories, Crawford Hill Laboratory, Box 400, Holmdel, NJ 07733, Rm. L-121.

[1]Carlo Cercignani, *Theory and Application of the Boltzmann Equation* (Elsevier, New York, 1975).

[2]S. Chapman and T. G. Cowling, *The Mathematical Theory of Nonuniform Gases* (Cambridge University Press, Cambridge, 1960).

[3]Poul Daul, *Introduction to Electron and Ion Optics* (Academic, New York, 1973).

[4]T. E. Darcie, M.A.Sc. thesis, University of Toronto, 1979 (unpublished).

[5]M. M. R. Williams, *Mathematical Methods in Transport Theory* (Butterworths, London, 1971).

[6]F. B. Pidduck, Proc. London Mathematical Soc. **15**, 8 (1915).

[7]A. L. Viehland and E. A. Mason, Ann. Phys. **91**, 499 (1975).

[8]G. H. Wannier, Bell System Tech. J. **32**, 170 (1953).

[9]G. L. Braglia, Beitr. Plasmaphys. **20**, 147 (1980).

[10]H. Grad, *Encyclopedia of Physics,* edited by S. Flugge (Springer, Berlin, 1958), Vol. 12, p. 205.

[11]V. C. Boffi and V. G. Molinari, Nuovo Cimento **34b**, 345 (1976).

[12]V. C. Boffi and V. G. Molinari, Nuovo Cimento **49b**, 77 (1979).

[13]V. C. Boffi, V. G. Molinari, and W. Wonnenberger, Nuovo Cimento **45b**, 109 (1978).

[14]J. Dorning, C. Pescatore, and G. Spiga, Rarefied Gas Dyn. Proc. Int. Symp. **51**, 745 (1976).

[15]S. Kuhn, Phys. Rev. A **22**, 2460 (1980).

[16]H. R. Skullerud and S. Kuhn, J. Phys. D **16**, 1225 (1983).

[17]H. R. Skullerud, J. Phys. B **6**, 728 (1973).

[18]G. N. Patterson, *Introduction to the Kinetic Theory of Gas Flows,* (University of Toronto Press, Toronto, 1971).

[19]T. E. Darcie, University of Toronto Institute of Aerospace Studies, Report No. UTIAS-269 (1982) (unpublished).

[20]Y. A. Kovalenko and V. P. Shumilin, Zh. Tekh. Fiz. **49**, 969 (1979) [Sov. Phys. Tech. Phys. **24(5)**, 569 (1979)].

[21]E. C. Whipple, Jr., Phys. Fluids **15(6)**, 988 (1972).

[22]B. B. Hamel and D. R. Willis, Phys. Fluids **9**, 829 (1966).

[23]F. Smithies, *Cambridge Tracts in Mathematics and Mathematical Physics,* (Cambridge University Press, Cambridge, 1958).

[24]F. B. Hildebrand, *Introduction to Numerical Analysis* (McGraw Hill, New York, 1956).

[25]Z. Kopal, *Numerical Analysis* (Wiley, New York, 1955).

[26]J. B. French, *Molecular Beams for Rarefied Gasdynamic Research,* NATO AGARDograph No. 112 (AGARD, Paris, 1966), p. 112.